

Cryo-EM structure of AAV8 and epitope mapping of CaptureSelect AAVX

Authors

Ieva Drulyte¹, Hans Raaijmakers¹, Pim Hermans², Hendrik Adams² and Mazdak Radjainia¹

¹Materials and Structural Analysis Division, Thermo Fisher Scientific, Eindhoven, Netherlands; ²Purification and Pharma Analytics, Thermo Fisher Scientific, Leiden, Netherlands

Keywords

AAV, cryo-EM, epitope mapping, CaptureSelect, AAVX, gene therapy, large-scale purification, empty/full analysis, QC, vector engineering, immunogenicity, tropism

Introduction

Viral-vector gene therapies for the treatment of genetic diseases are rapidly emerging and come with the promise to transform medical practice¹. Viral-vector gene therapy uses viruses as delivery vehicles for introducing genetic materials into a patient's cells. Adeno-associated viruses (AAVs) are an important class within the viral vector toolbox featuring wide-ranging tropism that enables targeting the central nervous system, eyes, liver, heart, and muscle¹. AAVs are also used for CRISPR/Cas genome editing systems². However, despite the significant momentum, several challenges need to be overcome before viral-vector gene therapies can live up to their promise. This includes optimization of the capsids as well as the production of viruses so that their efficacy and safety improve¹.

Exposure to naturally occurring AAV serotypes can lead to pre-existing immunity against viral capsids and their clearance, limiting the efficacy of a gene therapy³. Immunity to AAV can also be acquired by treatment, making repeat dosing or future gene therapies difficult. To make AAVs stealthier and escape clearance by neutralizing antibodies, their capsid surfaces can be mutated⁴. Engineering capsid surfaces can also improve the tissue-specificity of AAVs⁵. If tissue-specificity is low, higher dosing of virus particles is required, which in turn increases immune reactions and adverse outcomes⁶. Controlling the quality of AAV production is another important variable that plays into dosing. AAVs can assemble without their genetic payload and appear as empty capsids. Empty capsids increase the antigenic load without contributing to a clinical benefit. In addition, empty capsids may even carry hazardous impurities⁶.

In this white paper, we show that cryo-EM has two important applications in the development of AAV therapies. First, we demonstrate how simple 2D cryo-EM imaging can support the continuous quality assurance of AAVs by visualizing the ratio of empty and full capsids. Second, we exemplify the use of 3D cryo-EM structures in capsid engineering. We determined the 2.3 Å resolution cryo-EM structures of full and

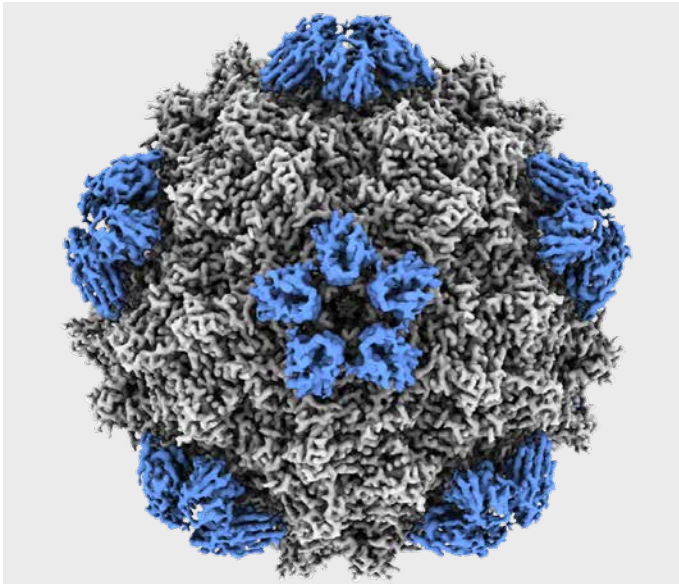


Figure 1 –Cryo-EM reconstruction of the full AAV8-AAVX complex. The capsid is colored grey, while the AAVX monomers bound to the 5-fold axis are colored blue.

empty AAV8 in complex with single-domain antibody fragment CaptureSelect™ AAVX (Figure 1). This antibody fragment is the ligand in Thermo Fisher's POROS™ CaptureSelect™ AAVX affinity resin enabling large-scale AAV purification of a broad range of naturally occurring or synthetic AAV serotypes. Using the structures for epitope mapping of AAVX, we identified which amino acid residues of the capsid are needed for AAVX-mediated purification, thereby informing the design of next-generation capsids.

Direct visualizations of empty and full capsids

Cryo-EM involves rapid freezing of AAV suspensions on a perforated sample carrier (i.e. 3 mm copper grid) and visualizing the sample using a cryogenic transmission electron microscope

(cryo-TEM), which shows the projections of AAV particles. In other words, the inside of AAVs can be seen. This enables us to determine whether an AAV particle is genome-filled or empty (Figure 2). Genome-filled capsids are characterized by being dark throughout. Empty capsids have dark boundaries at particle edges but are light in the center. Other sample properties like particle uniformity, integrity and clumping are also readily discerned. Non-specialists can be trained in a short amount of time to perform the microscopy and analysis of such an experiment. The empty and full AAV8 particles that we sourced show a high ratio of empty or full capsids, respectively. We were therefore able to visualize both empty and full AAV8 capsids in complex with the Thermo Scientific™ CaptureSelect™ AAVX ligand.

High-resolution 3D structures of AAV8/AAVX complexes Single-particle analysis of CaptureSelect™ AAVX-bound AAV8

The purified full and empty capsids of AAV8 were mixed with the ~14-kDa CaptureSelect AAVX affinity ligand at a ratio of 1:600 (capsid/affinity ligand) to ensure saturated binding. Complexes were incubated for 30 minutes at 4°C before sample vitrification.

AAV8-AAVX sample was applied to glow-discharged (20 mAmp, 30 seconds, Quorum GloQube) Quantifoil R1.2/1.3 grids overlaid with ultrathin 2 nm carbon, blotted for 4 seconds using blot force 0 and plunge frozen into liquid ethane using the Thermo Scientific™ Vitrobot™ Mark IV. The data were collected on a Glacios™ Cryo Transmission Electron Microscope (Cryo-TEM) equipped with a Selectris™ X Imaging Filter and Falcon™ 4 Direct Electron Detector camera operated in Electron-Event representation (EER) mode.

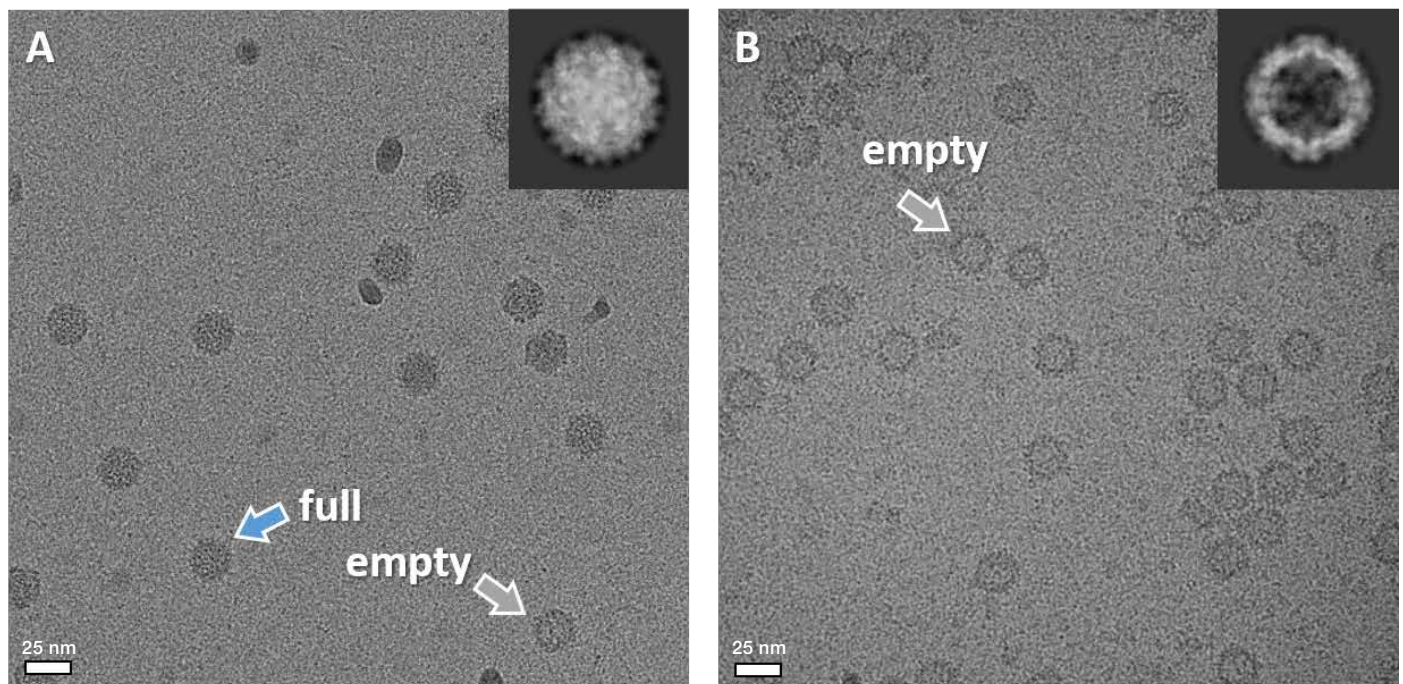
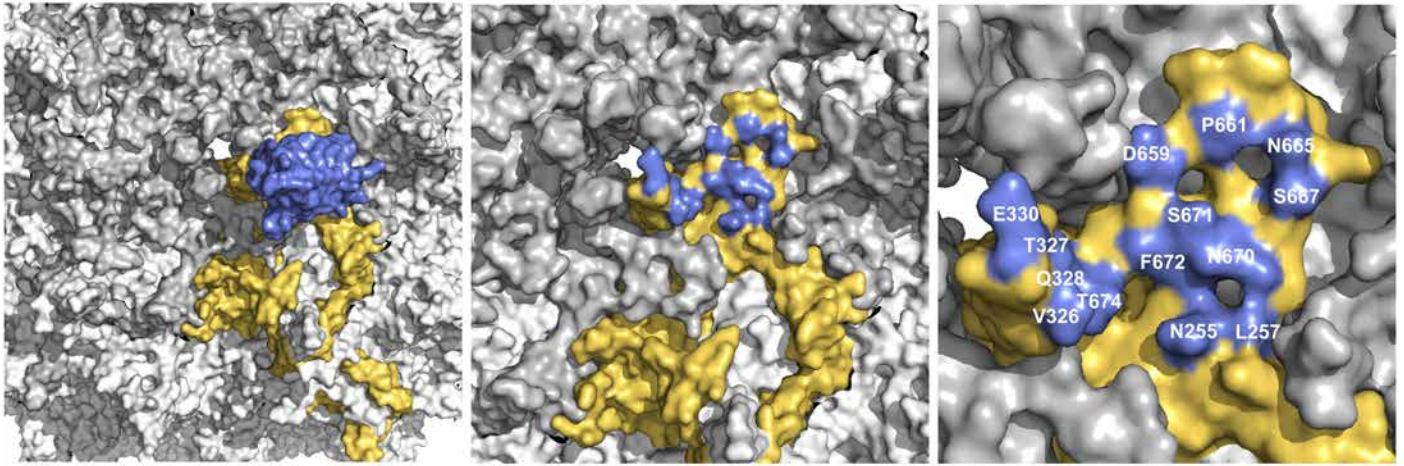


Figure 2 –Cryo-EM images and representative 2D class averages showing examples of full and empty AAV8-AAVX particles. (A) Representative micrograph and 2D class average of full AAV8-AAVX complex. Cryo-EM images show that a small proportion of this sample consists of empty particles. (B) Representative micrograph and 2D class average of empty AAV8-AAVX.



MAADGYLPDWLEDNLSEGIREWALKPGAPKPKANQQKQDDGRGLVLPGYKYLGFNGLDKGEFVNAADAAALEHDKAYDQQLQAGDNPYLRYNHADADEFQERLQEDTSFGGNL
 GRAVFOAKKRVLPEPLGLVEEGAKTAPGKKRPVEPSPQRS PDSSTGIGKKGQQPARKRLNFGQTDSESVDPQPLGEPAPSPGVGPNMTAAGGGAPMADNEGADGVGSSGN
 WHCDSTWLGDRVITTSRTWALPTYNNHLYKQISNGTSGGATNDNTYFGYSTPWGYFDNRFHCHFSPRDWQRLINNNWGFPRKRLSEKLFNIQVKEVTONNEGTKTIANNLTST
 IQVFTDSEYQLPYVLGSAHQGCLPPFPADVFMI PQYGYLTLNNGSQAVGRSSFYCLEYFPSQMLRTGNNFQFTYTFEDVFPFHSSYAHQSGLDRLMNP LI DQYLYLSRTQTGG
 TANTQTLGFSQGGPNTMANQAKNWLPGPCYRQQRVSTTTGQNNNSNFAWTAGTKYHLNGRNSLANPGIAMATHKDEERFFPSNGILIFGKQNAARDNADYSVMLTSEEEIKT
 TNPVATEEYGVADNLQQONTAPQIGTVNSQALPGMVWQNRDVYLGPIWAKIPHTDGNFHPSPLMGGFGLKHPFPQILIKNTPVPADPPTTFNOSKLNSEFIQYSTGQVSVS
 IEWELQKENSKRWNPEIQYTSNYYKSTSVDFAVNTEGVYSEPRPIGTRYLTRNL

Figure 3 –Left, AAVX binds to the capsid’s five-fold axis. One capsid protein is colored yellow, and the bound AAVX is colored blue. Middle, AAV8 surface is colored blue where an AAV8 residue is closer than 4 Å to AAVX. Right, epitope mapping for AAVX shows that AAVX interacts with one AAV8 subunit, and the epitope comprises short amino acid stretches on four loops.

The EPU Multigrad feature of the Thermo Scientific™ EPU Software was used to facilitate unattended data screening and collection of AAV8-AAVX samples.

Data processing was performed in the Relion 3 single particle analysis suite⁷. After motion- and CTF-correction, particles were picked and 2D classified. Particles from 2D classes with high-resolution detail were picked and refined with I1 symmetry imposed. After initial refinement, CTF refinement and 3D classification with no alignments (C1 symmetry) were used to further improve the resolution. Following global refinement, a mask was made encompassing five capsid proteins with bound AAVX molecules around the 5-fold axis of the capsid. Particles from the final global refinement were symmetry expanded, and focused classification was performed with the custom mask around the five-fold axis to further improve the resolution at the AAV8 and AAVX interaction interface.

Structural comparison of empty and full structures

In line with published AAV8 cryo-EM structures⁸, we did not observe major structural differences between empty or full particles reconstructions. We, therefore, deem the two structures equivalent for epitope mapping purposes. Epitope mapping was performed using the structure of full particles due to higher relevance for therapeutic purposes.

Epitope mapping of CaptureSelect AAVX

The cryo-EM map of AAV8 shows additional densities corresponding to AAVX, revealing its exact binding site. The epitope is located at the capsid’s five-fold axis and shows five bound AAVX particles (Figure 1). For epitope mapping, AAV8 contact residues were defined as amino acids located at ≤ 4.0 Å away from AAVX. AAVX recognizes three different loops of AAV8 (Figure 3). Specifically, AAVX interactions map to a conformational epitope corresponding to capsid residues N255-L257, V326-E330, and D659- T674. These stretches are very small and spread across the entire AAV8 sequence, highlighting the precision and complete view that cryo-EM affords to epitope mapping. Furthermore, we compared contact residues of AAV8 to sequences of other AAV serotypes (Figure 4). AAVX epitope residues map to capsid regions that are largely conserved between serotypes, which is why AAVX can be used for the purification of different AAV serotypes.

	255-257	326-330	659-674
AAV8	PTYN NHLYKQI	QVKE VTON EGTKT	PVPAD PPTTFNOSKLNSEFI TQYST
AAV1	PTYN NHLYKQI	QVKE VT TNDGVTT	PVPAN PPAEFSATKFASEFI TQYST
AAV2	PTYN NHLYKQI	QVKE VTON DGTTT	PVPAN PSTTFSAAKFASEFI TQYST
AAV3	PTYN NHLYKQI	QVRG VTON DGTTT	PVPAN PEFTTSPAKFASEFI TQYST
AAV4	PTYN NHLYKRL	QVKE VT TSNGETT	PVPAN PATTFSTPVSSEFI TQYST
AAV5	PSY NHQYREI	QVKE VTVQ DSTTT	PVPG NI-TSFS DVPV SSSEFI TQYST
AAV6	PTYN NHLYKQI	QVKE VT TNDGVTT	PVPAN PPAEFSATKFASEFI TQYST
AAV7	PTYN NHLYKQI	QVKE VT TNDGVTT	PVPAN PEVFTPAKFASEFI TQYST
AAV9	PTYN NHLYKQI	QVKE VT DNNGVKT	PVPAD PPPTAFNKDKLNSEFI TQYST
AAV10	PTYN NHLYKQI	QVKE VTON EGTKT	PVPAD PPTTFSQAKLASEFI TQYST

Figure 4 – Sequence alignment of AAV serotypes with AAVX contact residues highlighted in blue.

Discussion

There is pressure on gene therapy companies to improve AAVs in regards to tropism, immune clearance as well as large-scale production⁹, so that their dosing and associated side-effects can be reduced. Our results show that cryo-EM is a versatile tool for supporting these goals and a variety of gene therapy teams.

2D cryo-EM imaging doesn't require special expertise and can visualize the ratio of empty/full AAV particles, the presence of partially filled particles, aggregation state, or other particle morphology related particle characteristics. Additionally, cryo-EM has a unique ability to rapidly determine the high-resolution 3D structures of AAVs without the need for crystals, creating a rational basis for capsid engineering. The robustness and predictability of AAV structure determination by cryo-EM is therefore well suited for comparative structural analyses of multiple vectors or ligands⁸.

Structure-based capsid engineering has the benefit of precision. Having an atomic-level understanding of the capsid enables us to guide the design of AAV variants with high accuracy. For example, our epitope mapping of CaptureSelect AAVX ligand establishes which residues can and cannot be altered on AAVs if this affinity resin is being used for large-scale production. Another AAV epitope mapping use case is to characterize neutralizing antibodies of patients and determine an atlas of antigenic hotspots. Such atlases can then guide capsid modifications that escape antibody responses and help create an arsenal of AAV gene delivery stealth vehicles¹⁰.

In summary, cryo-EM is ideally suited to help overcome a subset of gene therapy core challenges.

References

1. Bulcha JT, Wang Y, Ma H, Tai PWL, Gao G. *Viral vector platforms within the gene therapy landscape*. Signal Transduct Target Ther. 2021 Feb 8; 6(1):53.
2. Falese L, Sandza K, Yates B, Triffault S, Gangar S, Long B, Tsuruda L, Carter B, Vettermann C, Zoog SJ, Fong S. *Strategy to detect pre-existing immunity to AAV gene therapy*. Gene Ther. 2017 Dec; 24(12):768-778.
3. Zhu FC, Guan XH, Li YH, Huang JY, Jiang T, Hou LH, Li JX, Yang BF, Wang L, Wang WJ, Wu SP, Wang Z, Wu XH, Xu JJ, Zhang Z, Jia SY, Wang BS, Hu Y, Liu JJ, Zhang J, Qian XA, Li Q, Pan HX, Jiang HD, Deng P, Gou JB, Wang XW, Wang XH, Chen W. *Immunogenicity and safety of a recombinant adenovirus type-5-vectored COVID-19 vaccine in healthy adults aged 18 years or older: a randomised, double-blind, placebo-controlled, phase 2 trial*. Lancet. 2020 Aug 15; 396(10249):479-488.
4. Barnes C, Scheideler O, Schaffer D. *Engineering the AAV capsid to evade immune responses*. Curr Opin Biotechnol. 2019 Dec; 60:99-103.
5. Wang D, Li S, Gessler DJ, Xie J, Zhong L, Li J, Tran K, Van Vliet K, Ren L, Su Q, He R, Goetzmann JE, Flotte TR, Agbandje-McKenna M, Gao G. *A Rationally Engineered Capsid Variant of AAV9 for Systemic CNS-Directed and Peripheral Tissue-Detargeted Gene Delivery in Neonates*. Mol Ther Methods Clin Dev. 2018 Mar 16; 9:234-246.
6. Mullard A. *Gene therapy community grapples with toxicity issues, as pipeline matures*. Nat Rev Drug Discov. 2021 Nov; 20(11):804-805
7. Zivanov J, Nakane T, Forsberg BO, Kimanius D, Hagen WJ, Lindahl E, Scheres SH. *New tools for automated high-resolution cryo-EM structure determination in RELION-3*. Elife. 2018 Nov 9; 7:e42166.
8. Mietzsch M, Barnes C, Hull JA, Chipman P, Xie J, Bhattacharya N, Sousa D, McKenna R, Gao G, Agbandje-McKenna M. *Comparative Analysis of the Capsid Structures of AAVrh.10, AAVrh.39, and AAV8*. J Virol. 2020 Feb 28; 94(6):e01769-19.
9. Li C, Samulski RJ. *Engineering adeno-associated virus vectors for gene therapy*. Nat Rev Genet. 2020 Apr; 21(4):255-272.
10. Smith JK, Agbandje-McKenna M. *Creating an arsenal of Adeno-associated virus (AAV) gene delivery stealth vehicles*. PLoS Pathog. 2018 May 3; 14(5):e1006929.

Learn more at
thermofisher.com/PharmaceuticalResearchUsingCryoEM